

Constraining the low-energy $S = -2$ meson-baryon interaction with two-particle correlations

V. Mantovani Sarti^{a,*}, A. Feijoo^{b,†}, I. Vidaña^{c,‡}, A. Ramos^{d,§}, F. Giacosa^{e,f}, T. Hyodo^{g,h}, Y. Kamiya^{i,h}

^a *Physik Department E62, Technische Universität München, Garching, Germany, EU**

^b *Instituto de Física Corpuscular, Centro Mixto Universidad de Valencia-CSIC, Institutos de Investigación de Paterna, Aptdo. 22085, E-46071 Valencia, Spain[†]*

^c *Istituto Nazionale di Fisica Nucleare, Sezione di Catania, Dipartimento di Fisica “Ettore Majorana”, Università di Catania, Via Santa Sofia 64, I-95123 Catania, Italy[‡]*

^d *Departament de Física Quàntica i Astrofísica and Institut de Ciències del Cosmos (ICCUB), Facultat de Física, Universitat de Barcelona, Barcelona, Spain[§]*

^e *Institute of Physics, Jan Kochanowski University, ul. Uniwersytecka 7, 25-406 Kielce, Poland*

^f *Institute of Theoretical Physics, Goethe University, Max-von-Laue-Str.1, 60438, Frankfurt am Main, Germany*

^g *Department of Physics, Tokyo Metropolitan University, Hachioji 192-0397, Japan*

^h *RIKEN Interdisciplinary Theoretical and Mathematical Science Program (iTHEMS), Wako 351-0198, Japan and*

ⁱ *Helmholtz-Institut für Strahlen- und Kernphysik and Bethe Center for Theoretical Physics, Universität Bonn, D-53115 Bonn, Germany*

The two-particle correlation technique applied to $K^- \Lambda$ pairs in pp collisions at LHC recently provided the most precise data on the strangeness $S = -2$ meson-baryon interaction. In this letter, we use for the first time femtoscopic data to constrain the parameters of a low-energy effective QCD Lagrangian. The tuned model delivers new insights on the molecular nature of the $\Xi(1620)$ and $\Xi(1690)$ states. This procedure opens the possibility to determine higher order corrections, directly constraining QCD effective models particularly in the multi-strange and charm sectors.

Introduction: The dynamics of the strong interaction between strange hadrons at low and intermediate energies is still a rather uncharted territory, both experimentally and theoretically. Namely, in this energy regime, a quantitative description of hadronic interactions in terms of the elementary quark and gluon degrees of freedom is hindered by the mathematical problems associated to the non-perturbative character of Quantum-Chromo-Dynamics (QCD). Effective Lagrangians, employing hadronic degrees of freedom and including the fundamental symmetries of QCD as well as spontaneous and anomalous breaking patterns, have been widely used to circumvent this difficulty since the pioneering work of Weinberg [1–3].

Amongst these effective approaches, Chiral Perturbation theory (χ PT) has proved to be an extremely powerful tool to compute in a systematic way many low-energy observables (e.g. cross-sections) and to provide insights on the underlying hadronic interactions. The χ PT framework allows us to investigate higher-order terms in the chiral expansion of the interaction, which can significantly improve the understanding of the underlying QCD dynamics in the system at hand. Each term in the Lagrangian is preceded by the so-called Low Energy Constants (LECs), parameters which are not fixed by the underlying theory and hence must be determined by a fit to the available experimental data.

In this work we focus on the $S = -2$ meson-baryon

interaction, dominated by the $\pi \Xi - \bar{K} \Lambda - \bar{K} \Sigma - \eta \Xi$ coupled-channel dynamics. Similarly to the $\Lambda(1405)$, a molecular $\pi \Sigma - \bar{K} N$ state arising from the interplay between these two coupled-channels [4–7], the $\Xi(1620)$ and $\Xi(1690)$ resonances might also be dynamically generated within the $S = -2$ meson-baryon interaction, thereby acquiring a molecular structure. In spite of the large theoretical effort devoted in the last two decades [8–13] to the understanding of the properties of the $\Xi(1620)$ and $\Xi(1690)$ states, a clear picture on their nature is still missing. Recently, the authors of Ref. [14] delivered the first unitarized effective meson-baryon chiral Lagrangian that includes contributions beyond the leading contact-term interaction in the $S = -2$ sector. The inclusion of higher orders in the chiral expansion reduced the disagreement between model predictions and the available experimental data on the two Ξ^* states, but it also introduced more LECs, namely more unknown parameters to be constrained from data. Unfortunately, current experimental information, which includes only evidence of the $\Xi(1690)$ resonance decaying into $K^- \Lambda$ [15–17] and the first observation of the neutral $\Xi(1620)$ decaying into $\pi^+ \Xi^-$ [18], is not sufficient to constrain the next-to-leading order (NLO) LECs. This limitation drove the authors of Ref. [14] to invoke $SU(3)$ flavour symmetry to adopt the same LECs of the meson-baryon interaction models in the $S = -1$ sector, which benefit from a much larger data sample [19–31]. Clearly, an improvement in the

theoretical developments on the $S = -2$ meson-baryon interaction requires new and more precise experimental data.

Such experimental input became available with the recent ALICE measurement of the $K^- \Lambda$ correlation function (CF) in pp collisions at $\sqrt{s} = 13$ TeV, which delivered the most precise data on this interaction and provided the first experimental observation of the $\Xi(1620)$ decaying into $K^- \Lambda$ pairs [32]. In the present study, these femtoscopic data is used for the first time to fit the parameters of the state-of-the-art χ PT effective Lagrangian at NLO [14]. The resulting unitarized χ PT (U χ PT) amplitudes are employed to investigate the position and couplings of the poles related to the $\Xi(1620)$ and $\Xi(1690)$ states to the different channels, leading to a complete new distribution of the molecular composition of these two resonances.

The results presented in this work make use of a novel method to constrain the low-energy QCD effective models for interactions involving multi-strange and charm hadrons, which cannot be accessed via traditional scattering experiments. For these interactions, correlation measurements at LHC already provided the experimental access to a large amount of two-body and three-body interactions [33–42]. In the future, thanks to the even larger statistics expected at LHC [43], and with brand new dedicated experiments [44], femtoscopic measurements will be the only data at our disposal able to directly constrain the two-body scattering amplitude, hence the methodology described in this Letter provides a tool to guide future comparisons with correlation data.

Formalism: In the case of a multi-channel system, such as the one we are considering in this work, the corresponding two-particle CF of a given observed channel i (e.g. $K^- \Lambda$) reads [45–47]

$$C_i(k^*) = \sum_j \omega_j^{\text{prod.}} \int d^3 r^* S_j(r^*) |\psi_{ji}(k^*, r^*)|^2. \quad (1)$$

Here k^* and r^* represent, respectively, the relative momentum and distance between the two particles, measured in the pair rest frame. The sum runs over the elastic ($j = i = K^- \Lambda$) and the inelastic channels ($j = \pi^- \Xi^0, \pi^0 \Xi^-, K^- \Sigma^0, \bar{K}^0 \Sigma^-, \eta \Xi^-$).

The contributions of the inelastic channels are scaled by the production weights $\omega_j^{\text{prod.}}$, which take into account how many j pairs, produced as initial states, can convert to the measured i final state. The emitting source $S_j(r^*)$ describes the probability of emitting the j pair at a relative distance r^* and, particularly in p-p femtoscopic measurements, might be different in each channel due to the feed-down from strongly de-

caying resonances, specific for each pair [39, 48, 49]. Finally, the last ingredient is the relative wave function $\psi_{ji}(k^*, r^*)$, embedding the strong interaction arising from the coupled-channel dynamics in the system. Following the formalism in [46], the wave functions can be obtained from the scattering amplitude.

The starting point from which we derive the scattering amplitude within the U χ PT is the chiral effective Lagrangian up to NLO $\mathcal{L}_{\phi B}^{eff} = \mathcal{L}_{\phi B}^{(1)} + \mathcal{L}_{\phi B}^{(2)}$, with

$$\mathcal{L}_{\phi B}^{(1)} = i \langle \bar{B} \gamma_\mu [D^\mu, B] \rangle - M_0 \langle \bar{B} B \rangle - \frac{1}{2} D \langle \bar{B} \gamma_\mu \gamma_5 \{u^\mu, B\} \rangle - \frac{1}{2} F \langle \bar{B} \gamma_\mu \gamma_5 [u^\mu, B] \rangle, \quad (2)$$

$$\mathcal{L}_{\phi B}^{(2)} = b_D \langle \bar{B} \chi_+, B \rangle + b_F \langle \bar{B} [\chi_+, B] \rangle + b_0 \langle \bar{B} B \rangle \langle \chi_+ \rangle + d_1 \langle \bar{B} \{u_\mu, [u^\mu, B]\} \rangle + d_2 \langle \bar{B} [u_\mu, [u^\mu, B]] \rangle + d_3 \langle \bar{B} u_\mu \rangle \langle u^\mu B \rangle + d_4 \langle \bar{B} B \rangle \langle u^\mu u_\mu \rangle. \quad (3)$$

The contact term, corresponding to the Weinberg-Tomozawa (WT) contribution, and the direct and crossed Born terms are included in $\mathcal{L}_{\phi B}^{(1)}$ whereas the tree-level NLO contributions are fully extracted from $\mathcal{L}_{\phi B}^{(2)}$. In these equations, B is the octet baryon matrix, while the matrix of the pseudoscalar mesons ϕ is implicitly contained in $u_\mu = iu^\dagger \partial_\mu U u^\dagger$, where $U(\phi) = u^2(\phi) = \exp\{\sqrt{2}i\phi/f\}$ with f being the effective meson decay constant. The covariant derivative is given by $[D_\mu, B] = \partial_\mu B + [\Gamma_\mu, B]$, with $\Gamma_\mu = [u^\dagger, \partial_\mu u]/2$, while $\chi_+ = 2B_0(u^\dagger \mathcal{M} u^\dagger + u \mathcal{M})$, with $\mathcal{M} = \text{diag}(m_u, m_d, m_s)$ and $B_0 = -\langle 0 | \bar{q}q | 0 \rangle / f^2$, is the explicit chiral symmetry breaking term. The values of the axial vector constants are taken as $D = 0.8$ and $F = 0.46$ and M_0 is the baryon octet mass in the chiral limit. The NLO Lagrangian depends on a few LECs, namely b_D, b_F, b_0 and d_i ($i = 1, \dots, 4$), to be determined here from the fit to the measured $K^- \Lambda$ correlation.

The total interaction kernel up to NLO, derived from Eqs. (2) and (3), reads $V_{ij} = V_{ij}^{WT} + V_{ij}^D + V_{ij}^C + V_{ij}^{NLO}$, where the elements of the interaction matrix \hat{V}_{ij} couple all possible meson-baryon channels, see Refs. [50, 51] for details. The interaction kernel in the present ($S = -2, Q = -1$) sector is derived from the ($S = -2, Q = 0$) one [14] by employing basic isospin arguments.

The final step is to connect the interaction kernel to the scattering amplitude T_{ij} , required to evaluate the wave functions and calculate the CF. The U χ PT method, adopted here due to the presence of the Ξ^* resonances, solves the Bethe-Salpeter equations through an on-shell factorization, leaving a simple system of algebraic equations expressed in matrix form as

$$T_{ij} = (1 - V_{il} G_l)^{-1} V_{lj}, \quad (4)$$

being G_l the meson-baryon loop function whose loga-

rithmic divergence is handled by dimensional regularization

$$G_l = \frac{2M_l}{(4\pi)^2} \left\{ a_l(\mu) + \ln \frac{M_l^2}{\mu^2} + \frac{m_l^2 - M_l^2 + s}{2s} \ln \frac{m_l^2}{M_l^2} + \frac{q_{\text{cm}}}{\sqrt{s}} \ln \left[\frac{(s + 2\sqrt{s}q_{\text{cm}})^2 - (M_l^2 - m_l^2)^2}{(s - 2\sqrt{s}q_{\text{cm}})^2 - (M_l^2 - m_l^2)^2} \right] \right\}. \quad (5)$$

The former expression comes in terms of the baryon (M_l) and meson (m_l) masses for the l -channel as well as the subtraction constants (SCs) a_l , replacing the divergence for a given dimensional regularization scale μ , taken to be 1 GeV. Despite a natural size can be established for them, the lack of knowledge about the SCs requires their inclusion in the fitting procedure. The number of independent SCs is four following isospin symmetry arguments. Summarizing, the $U\chi\text{PT}$ with WT+Born+NLO terms in this sector leaves a scattering amplitude that depends on 13 parameters never determined before. Hence, the $K^- \Lambda$ CF offers an unprecedented opportunity to constrain a theoretical model that can be employed to make novel predictions in a quite unknown sector.

The procedure to fit the LECs and SCs of this model, referred from now on as the Valencia–Barcelona–Catania (VBC) model, is described in the following section.

Fitting procedure: Following the approach in the experimental $K^- \Lambda$ analysis [32], the function we use to fit the data reads

$$C(k^*) = N_D \times C_{\text{model}}(k^*) \times C_{\text{background}}(k^*). \quad (6)$$

The term $C_{\text{model}}(k^*) = 1 + \lambda_{\text{gen}} \times (C_{\text{gen}}(k^*) - 1) + \sum_{\text{res}} \lambda_{\text{res}} \times (C_{\text{res}}(k^*) - 1)$ includes the genuine $K^- \Lambda$ correlation, defined via Eq. (1) and obtained within the VBC model, as well as the residual contributions. The correlations are weighted with the same λ parameters used in [32] and the interaction amongst the pairs composing the residual correlations is modeled using the same assumptions adopted in [32].

A prior knowledge of the source function is needed to evaluate both the genuine and residual contributions [45, 52]. In particular, to obtain $C_{\text{gen}}(k^*)$, we determined the specific emitting sources for each elastic and inelastic channel, following the same approach used in the treatment of the coupled-channel contributions of the $K^- p$ correlation in [39]. For the elastic $K^- \Lambda$ part, we assume the same double Gaussian source parametrization employed in [32]. The same source distribution is assumed also for the residual correlations.

As shown in [39], depending on the pairs entering

the inelastic contributions, the corresponding source profiles can significantly deviate from the elastic one. Such an effect is particularly relevant when pions are involved, as in the case at hand here in which the channels $\pi^- \Xi^0$ and $\pi^0 \Xi^-$ are present. We perform a detailed study on the source profiles of the inelastic channels by adopting the data-driven resonance source model (RSM) in [48], used as well in the $K^- \Lambda$ correlation measurement [32] and in several femtosopic analyses [34, 37, 39–42, 53]. Following [39], we build, for each inelastic channel, a total source having a Gaussian core with radius $r_{\text{core}} = 1.11 \pm 0.04$ [32], common to all channels, and a non-gaussian contribution from the feeding of strongly decaying resonances. As done for the elastic $K^- \Lambda$ channel, the final inelastic sources are modeled with a double Gaussian parametrization. Compatible parameters are found between the $K^- \Sigma^0$ and $\bar{K}^0 \Sigma^-$ effective sources and the $K^- \Lambda$ one, while larger radii are obtained for the $\pi \Xi$ channels due to the long-lived resonances ($c\tau \gtrsim 5$ fm) feeding to the pions. The remaining $S_{\eta \Xi^-}(r^*)$ distribution is localized at slightly smaller r^* since no significant strong feed-down to the Ξ baryon is present. We assign the same relative uncertainties ($\approx 4\%$) on the inelastic source's parameters of the reported one on r_{core} in [32].

The last quantities to be evaluated are the production weights $\omega_j^{\text{prod.}}$. We employed the same data-driven method used for the $K^- p$ correlation analysis [39], measured in the same high-multiplicity dataset we are considering. The values obtained for each inelastic channel (normalized to the $K^- \Lambda$ one, e.g. $\omega_{K^- \Lambda}^{\text{prod.}} = 1$) are $\omega_{\pi^- \Xi^0}^{\text{prod.}} = 1.53$, $\omega_{\pi^0 \Xi^-}^{\text{prod.}} = 1.58$, $\omega_{K^- \Sigma^0}^{\text{prod.}} = 0.68$, $\omega_{\bar{K}^0 \Sigma^-}^{\text{prod.}} = 0.63$ and $\omega_{\eta \Xi^-}^{\text{prod.}} = 0.18$. We associate errors on the productions weights of the order of maximum $\approx 10\%$ by propagating the available uncertainties on the parameters used to estimate the inelastic pairs yields [54] and the k^* kinematics, as done in [39]. Additional details on the source and $\omega_j^{\text{prod.}}$ determination can be found in the Supplemental Material.

For the comparison with the measured $K^- \Lambda$ correlation in [32], a residual background, given by the last term in Eq. (6), must be taken into account. The profile of $C_{\text{background}}(k^*)$, publicly available at [55], is composed of a polynomial function plus the presence of several resonances at large k^* , amongst which the $\Xi(1690)$. In [32], the latter has been modeled with a Breit-Wigner distribution and the corresponding mass and widths extracted from the fit were found compatible with the PDG values [56]. In our work, the $\Xi(1690)$ is dynamically generated within the VBC model entering the $C_{\text{model}}(k^*)$ term, hence the modeling of this resonance in the background should not be included. To do so, we perform a fit to the

available $C_{\text{background}}(k^*)$, using Eq. (3) in [32], and we set to zero the Breit-Wigner term for the $\Xi(1690)$. The final background correlation entering in our fit contains only as resonances the Ω at $k^* \approx 210$ MeV/ c and the $\Xi(1820)$ at $k^* \approx 400$ MeV/ c .

The fit of $C_{\text{tot}}(k^*)$ to the $K^- \Lambda$ correlation data is performed, as in [32], in the range $0 \leq k^* \leq 500$ MeV/ c , leaving as free parameters the normalization constant N_D , the LECs and SCs of the VBC model. The fitting procedure we adopt is based on the bootstrap technique used as in [32]. A total of 1000 samplings is performed in which we also, at each iteration, vary randomly the values of the source parameters and production weights within the quoted uncertainties.

Results: In Fig. 1 we present in the upper panel the results of the fit of $C(k^*)$ (red bands) to the measured $K^- \Lambda$ correlation. In the lower panel we estimate for each k^* interval the agreement between the data and the model (normalized to the statistical error of the data), expressed in terms of numbers of standard deviation ($n\sigma$). In the considered k^* range the average $n\sigma$ is around 1.3, confirming the agreement between the femtoscopic data and the tuned VBC model.

The extracted parameters of the VBC model are shown in Tab. I. Values of the SCs of ~ -2 are of ‘natural size’ [57]. The lowest-order LEC f tends towards its smallest allowed value, f_π . The NLO LECs are, in general, comparable in size with those determined for the $S = -1$ interaction [58–60], with the exception of b_0 , whose size turns out to be roughly one order of magnitude larger. As this parameter appears in all the diagonal elements of the NLO D_{ij} coefficients (see Table 1 in [14] and Eq. (10) in [51]), it is responsible for the generation of moderately attractive interactions in the $K^- \Lambda$ and $\eta \Xi^-$ channels that are otherwise null at the WT level. This provides the $S = -2$ model at NLO with a richer coupled-channel structure than its LO counterpart, allowing it to reproduce the CF in a wide momentum range. Indeed, the tuned VBC model describes the data very well in the region of $k^* \leq 200$ MeV/ c , where the presence of the $\Xi(1620)$, dynamically generated as a meson-baryon quasi-bound state in the model, is dominant. A reasonable description is also found for the peak around $k^* \approx 250$ MeV/ c associated to the $\Xi(1690)$ state, which is also generated dynamically by the VBC model.

In Table II we present the pole properties for the $\Xi(1620)$ and $\Xi(1690)$ states obtained in the VBC model. Both poles are found in the physically relevant Riemann sheet and the corresponding masses and widths are compatible with the current experimental data [15, 18],

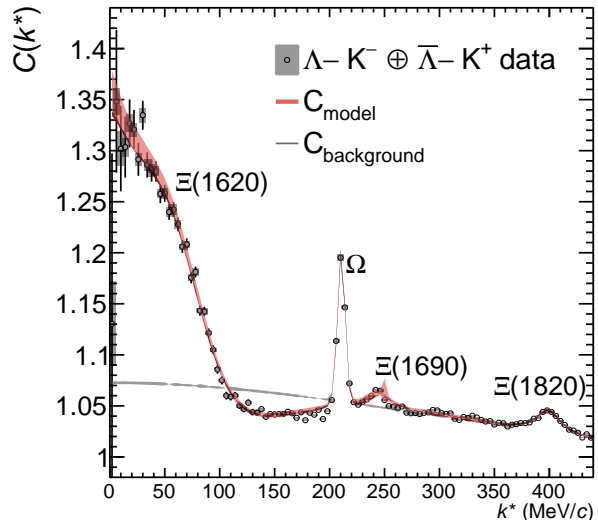


Figure 1. Upper panel: Experimental $K^- \Lambda$ correlation data with systematic (gray boxes) and statistical (vertical lines) uncertainties [32]. The red band is the total fit obtained with the VBC model. The darker shade is due to the statistical uncertainty on the data, while the light shade corresponds to the total error $\sigma_{\text{tot}} = \sqrt{\sigma_{\text{stat}}^2 + \sigma_{\text{syst}}^2}$. The gray band represents the background. Lower panel: deviation between data and model in terms of numbers of standard deviations.

reported in the last two rows. Such an agreement confirms, as demonstrated in [14] and in contrast to all previous studies [8–13], that the inclusion of Born and the NLO contributions is crucial to dynamically generate both Ξ^* simultaneously. A novel aspect of the present study comes when inspecting the couplings g_i of the different channels to the $\Xi(1620)$ pole. The strong coupling to the highest channel, at the expense of reducing sizeably the ones to the $\pi \Xi$ and $K^- \Lambda$, reveals a paradigm shift in the compositeness of the $\Xi(1620)$ state. All former works interpret such a state as a $\pi \Xi^- \bar{K} \Lambda$ molecule with a non-negligible coupling to the $\bar{K} \Sigma$ channel. In the present study, the molecule basically consists of a $K^- \Lambda - \eta \Xi^-$ mixing, with the latter being the dominant component. A direct consequence of the reduced couplings to the $\pi \Xi$ and $K^- \Lambda$ open channels is a much narrower $\Xi(1620)$ width, in contrast to previous values, which approaches the experimental data. For the $\Xi(1690)$ resonance, which appears basically as a $\bar{K} \Sigma$ quasi-bound state, we observe that the theoretical energy is located below the expected experimental value and the lowest $\bar{K} \Sigma$ threshold. The latter condition reduces the possibility of decaying into $K^- \Sigma^0$ states, leading to a reduction of the width with respect to [14].

Table I. Extracted fit parameters with LECs and subtraction constants of the VBC $S = -2$ meson-baryon interaction at NLO and normalization constant N_D . The bootstrap method [61–63] was employed to determine the errors of the parameters.

$a_{\Xi\pi}$	-2.96 ± 0.11
$a_{\Lambda\bar{K}}$	-1.87 ± 0.10
$a_{\Sigma\bar{K}}$	-1.32 ± 0.02
$a_{\Xi\eta}$	-2.42 ± 0.03
f/f_π	1.000 ± 0.001
b_0 [GeV $^{-1}$]	-2.997 ± 0.002
b_D [GeV $^{-1}$]	1.20 ± 0.09
b_F [GeV $^{-1}$]	-0.30 ± 0.12
d_1 [GeV $^{-1}$]	-0.69 ± 0.18
d_2 [GeV $^{-1}$]	-0.21 ± 0.06
d_3 [GeV $^{-1}$]	0.08 ± 0.20
d_4 [GeV $^{-1}$]	-0.39 ± 0.05
N_D	1.0015 ± 0.0004

Table II. Poles, couplings and compositeness of the resonances generated by the VBC $S = -2$ meson-baryon interaction at NLO. The number between brackets in the first column denotes the channel threshold energy in MeV.

mass M :	1612.68 MeV	1670.28 MeV		
width Γ :	24.57 MeV	7.44 MeV		
Riemann sheet:	(---+++)	(---+++)		
	$ g_i $	$ g_i^2 dG/dE $	$ g_i $	$ g_i^2 dG/dE $
$\pi^-\Xi^0(1454)$	0.51	0.014	0.22	0.002
$\pi^0\Xi^-(1456)$	0.36	0.007	0.39	0.007
$K^-\Lambda(1609)$	0.94	0.162	0.07	0.000
$K^-\Sigma^0(1686)$	0.17	0.002	2.20	0.761
$\bar{K}^0\Sigma^-(1695)$	0.21	0.003	1.37	0.230
$\eta\Xi^-(1868)$	5.86	0.937	0.05	0.000
Experimental Ξ^* :	$\Xi(1620)$ [18]	$\Xi(1690)$ [56]		
mass M :	$1610.4 \pm 6.0_{-3.5}^{+5.9}$ MeV	1690 ± 10 MeV		
width Γ :	$59.9 \pm 4.8_{-3.0}^{+2.8}$ MeV	20 ± 15 MeV		

A good quality fit to the CF at low momenta can also be obtained with the simpler WT model at the expense of some SCs being close to zero and thus being rather ‘unnatural’. The resulting amplitudes present a low energy pole compatible with the lower one of the NLO fit. However, the WT model fails at describing the data around $k^* \sim 250$ MeV/c since no higher energy pole is generated.

Two important observations can be drawn: first, the information encoded in the CF strongly indicates the

existence of a resonance having an energy of around 1620 MeV and a width of $\lesssim 30$ MeV, as its shape can only be reproduced by an explicit inclusion of the resonance [32], or by theoretical models that generate it dynamically with similar characteristics. Secondly, it is necessary to implement the NLO terms of the chiral Lagrangian in order to reproduce the low momenta region of the CF and the $\Xi(1690)$ at $k^* \sim 250$ MeV/c. The position of the near-threshold $\Xi(1620)$ pole is related to the scattering length f_0 and effective range r_e [13, 64–66]. The tuned VBC model delivers respectively $f_0 = (0.23 \pm 0.05) + i(0.45 \pm 0.07)$ fm and $r_{\text{eff}} = (-6.35 \pm 5.57) + i(36.22 \pm 3.90)$ fm, in agreement with the results obtained within a more phenomenological approach in [32].

It is known that a near-threshold resonance above the threshold requires an important contribution from the effective range [13, 66], as it is the case of the $\Xi(1620)$ pole with the present model. With the scattering length only, the pole position is estimated as $M - i\Gamma/2 = 1739.83 + i180.53$ MeV, largely deviating from the values in Table II. The situation improves by including the effective range correction, $M - i\Gamma/2 = 1616.31 + i1.75$ MeV. The importance of r_e , having a larger magnitude than f_0 , is due to the location of the $\Xi(1620)$ pole above the $K^-\Lambda$ threshold. Interestingly, one can also repeat the study of Ref. [32] by using the same phenomenological Sill energy line-shape of Ref. [67] extended to all the six channels studied in this work. The pole for $\Xi(1620)$ in the $(-, -, -, +++)$ Riemann sheet reads $1617.4 - i3.6$ MeV, compatible with (but smaller than) the VBC results.

Conclusions: In this letter, we determined for the first time the LECs, up to higher-order corrections, of a state-of-the-art effective Lagrangian from high-precision femtosopic data. In particular, we focused on the $S = -2$ meson-baryon sector and use, as experimental constraints, the measured $K^-\Lambda$ correlation by ALICE [32]. The description of the data is based on a $U\chi$ PT NLO Lagrangian, which accounts for the full $(S = -2, Q = -1)$ meson-baryon coupled channel dynamics and dynamically generates the $\Xi(1620)$ and $\Xi(1690)$ states [14]. Effects of the inelastic channels on the calculated $K^-\Lambda$ CF were carefully taken into account with a data-driven estimation on the emitting source parameters and production weights.

The VBC model delivers a very good description of the data in the considered k^* range. The extracted SCs take their ‘natural size’ values and we observe a large sensitivity of the correlation data to the NLO LECs responsible for the elastic transitions.

The fitted parameters were used to study of the $\Xi(1620)$ and $\Xi(1690)$ poles, whose masses and widths turned out to be compatible with the available experimental measurements. As a novel effect of the femtosopic constraints and in contrast to previous calculations, one of the molecular states generated ($\Xi(1620)$) mainly consist of a $\eta\Xi$ quasi-bound state.

The method presented here can be extended to other interactions, involving strange and charm hadrons, which may potentially generate states from coupled channel dynamics, such as the $\Xi(1620)$ and $\Xi(1690)$ ones in the present study. For these cases the synergy between the theoretical modeling and available femtosopic data can provide complementary information on the nature of such exotic states.

ACKNOWLEDGEMENTS

This work was supported by the ORIGINS cluster DFG under Germany's Excellence Strategy - EXC2094 - 390783311 and the DFG through Grant SFB 1258 "Neutrinos and Dark Matter in Astro and Particle Physics". V. M. S. is supported by the Deutsche Forschungsgemeinschaft (DFG) through the grant MA 8660/1 - 1. This work was also supported by the Spanish Ministerio de Ciencia e Innovación (MICINN) and European FEDER funds under Contracts CEX2019-000918-M, PID2020-112777GB-I00, PID2020-118758GB-I00 and by Generalitat Valenciana under contract PROMETEO/2020/023. This project has received funding from the European Union Horizon 2020 research and innovation programme under the program H2020-INFRAIA-2018-1, grant agreement No.824093 of the STRONG-2020 project. A.F. is supported through Generalitat Valencia (GVA) Grant APOSTD-2021-112. This work has been supported in part by the Grants-in-Aid for Scientific Research from JSPS (Grant No. JP22K03637, No. JP19H05150, No. JP18H05402). F.G. acknowledges support from the *Polish National Science Centre* (NCN) through the *OPUS* project 2019/33/B/ST2/00613. This work was also supported by the DFG (Project number 196253076 - TRR 110) and the NSFC (Grant No. 11621131001) through the funds provided to the Sino-German CRC 110 "Symmetries and the Emergence of Structure in QCD"

- [1] S. Weinberg, "Phenomenological Lagrangians", *Physica A* **96** no. 1-2, (1979) 327–340.
- [2] S. Weinberg, "Nuclear forces from chiral lagrangians", *Phys. Lett. B* **251** (1990) 288–292.
- [3] S. Weinberg, "Effective chiral lagrangians for nucleon-pion interactions and nuclear forces", *Nucl. Phys. B* **363** (1991) 3–18.
- [4] T. Hyodo and D. Jido, "The nature of the $\Lambda(1405)$ resonance in chiral dynamics", *Prog. Part. Nucl. Phys.* **67** (2012) 55–98, [arXiv:1104.4474 \[nucl-th\]](#).
- [5] U.-G. Meißner, "Two-pole structures in QCD: Facts, not fantasy!", *Symmetry* **12** no. 6, (2020) 981, [arXiv:2005.06909 \[hep-ph\]](#).
- [6] M. Mai, "Review of the $\Lambda(1405)$ A curious case of a strangeness resonance", *Eur. Phys. J. ST* **230** no. 6, (2021) 1593–1607, [arXiv:2010.00056 \[nucl-th\]](#).
- [7] T. Hyodo and M. Niiyama, "QCD and the strange baryon spectrum", *Prog. Part. Nucl. Phys.* **120** (2021) 103868, [arXiv:2010.07592 \[hep-ph\]](#).
- [8] A. Ramos, E. Oset, and C. Bennhold, "On the spin, parity and nature of the $\Xi(1620)$ resonance", *Phys. Rev. Lett.* **89** (2002) 252001.
- [9] C. Garcia-Recio, M. F. M. Lutz, and J. Nieves, "Quark mass dependence of s wave baryon resonances", *Phys. Lett. B* **582** (2004) 49–54, [arXiv:nucl-th/0305100](#).
- [10] D. Gamermann, C. Garcia-Recio, J. Nieves, and L. L. Salcedo, "Odd Parity Light Baryon Resonances", *Phys. Rev. D* **84** (2011) 056017, [arXiv:1104.2737 \[hep-ph\]](#).
- [11] T. Sekihara, " $\Xi(1690)$ as a $\bar{K}\Sigma$ molecular state", *PTEP* **2015** no. 9, (2015) 091D01, [arXiv:1505.02849 \[hep-ph\]](#).
- [12] K. P. Khemchandani, A. Martínez Torres, A. Hosaka, H. Nagahiro, F. S. Navarra, and M. Nielsen, "Why $\Xi(1690)$ and $\Xi(2120)$ are so narrow?", *Phys. Rev. D* **97** no. 3, (2018) 034005, [arXiv:1608.07086 \[nucl-th\]](#).
- [13] T. Nishibuchi and T. Hyodo, "Analysis of $\Xi(1620)$ resonance and $\bar{K}\Lambda$ scattering length with chiral unitary approach", [arXiv:2305.10753 \[hep-ph\]](#).
- [14] A. Feijoo, V. Valcarce Cadenas, and V. K. Magas, "The $\Xi(1620)$ and $\Xi(1690)$ molecular states from $S=-2$ meson-baryon interaction up to next-to-leading order", *Phys. Lett. B* **841** (2023) 137927, [arXiv:2303.01323 \[hep-ph\]](#).
- [15] **LHCb** Collaboration, R. Aaij et al., "Evidence of a $J/\Psi\Lambda$ structure and observation of excited Ξ^- states in the $\Xi_b^- \rightarrow J/\Psi\Lambda K^-$ decay", *Sci. Bull.* **66** (2021) 1278.
- [16] **Belle** Collaboration, K. Abe et al., "Observation of Cabibbo suppressed and W exchange $\Lambda_{b,c}$ baryon decays", *Phys. Lett. B* **524** (2002) 33–43, [arXiv:hep-ex/0111032](#).
- [17] **BESIII** Collaboration, M. Ablikim et al., "Study of excited Ξ states in $\psi(3686) \rightarrow K^- \Lambda \bar{\Xi}^+ + c.c.$ ", [arXiv:2308.15206 \[hep-ex\]](#).
- [18] **BELLE** Collaboration, M. Sumihama et al., "Observation of $\Xi(1620)^0$ and $\Xi(1690)^0$ in $\Xi_c^+ \rightarrow \Xi^- \pi^+ \pi^+$ decays", *Phys. Rev. Lett.* **122** (2019) 072501.

* valentina.mantovani-sarti@tum.de

† edfeijoo@ific.uv.es

‡ isaac.vidana@ct.infn.it

§ ramos@fqa.ub.edu

- [19] W. E. Humphrey and R. R. Ross, “Low-energy interactions of K^- mesons in hydrogen”, *Phys. Rev.* **127** (1962) 1305–1323.
- [20] M. B. Watson, M. Ferro-Luzzi, and R. D. Tripp, “Analysis of $Y_0^*(1520)$ and determination of the Σ parity”, *Phys. Rev.* **131** (1963) 2248–2281.
- [21] T. S. Mast, M. Alston-Garnjost, R. O. Bangerter, A. S. Barbaro-Galtieri, F. T. Solmitz, and R. D. Tripp, “Elastic, Charge Exchange, and Total K^-p Cross-Sections in the Momentum Range 220-MeV/c to 470-MeV/c”, *Phys. Rev. D* **14** (1976) 13.
- [22] R. J. Nowak et al., “Charged Σ hyperon production by K^- meson interactions at rest”, *Nucl. Phys.* **B139** (1978) 61–71.
- [23] J. Ciborowski et al., “Kaon scattering and charged Σ hyperon production in K^-p interactions below 300 MeV/c”, *J. Phys.* **G8** (1982) 13–32.
- [24] M. Sakitt, T. B. Day, R. G. Glasser, N. Seeman, J. H. Friedman, W. E. Humphrey, and R. R. Ross, “Low-energy K^- meson interactions in Hydrogen”, *Phys. Rev.* **139** (1965) B719.
- [25] M. Bazzi et al., “A New Measurement of Kaonic Hydrogen X-rays”, *Phys. Lett. B* **704** (2011) 113.
- [26] M. Bazzi et al., “Kaonic hydrogen X-ray measurement in SIDDHARTA”, *Nucl. Phys. A* **881** (2012) 88.
- [27] V. K. Magas, E. Oset, and A. Ramos, “Evidence for the two pole structure of the $\Lambda(1405)$ resonance”, *Phys. Rev. Lett.* **95** (2005) 052301, [arXiv:hep-ph/0503043](#).
- [28] J. Siebenson and L. Fabbietti, “Investigation of the $\Lambda(1405)$ line shape observed in pp collisions”, *Phys. Rev. C* **88** (2013) 055201, [arXiv:1306.5183](#) [[nucl-ex](#)].
- [29] R. J. Hemingway, “Production of $\Lambda(1405)$ in K^-p reactions at 4.2 GeV/c”, *Nucl. Phys.* **B253** (1985) 742–752.
- [30] I. Zychor et al., “Shape of the $\Lambda(1405)$ hyperon measured through its $\Sigma^0\pi^0$ decay”, *Phys. Lett. B* **660** (2008) 167–171, [arXiv:0705.1039](#) [[nucl-ex](#)].
- [31] CLAS Collaboration, K. Moriya and R. Schumacher, “Properties of the $\Lambda(1405)$ measured at CLAS”, *Nucl. Phys.* **A835** (2010) 325–328, [arXiv:0911.2705](#) [[nucl-ex](#)].
- [32] ALICE Collaboration, S. Acharya et al., “Accessing the strong interaction between Λ baryons and charged kaons with the femtoscopy technique at the LHC”, *Phys. Lett. B* **845** (2023) 138145, [arXiv:2305.19093](#) [[nucl-ex](#)].
- [33] ALICE Collaboration, S. Acharya et al., “p-p, p- Λ and Λ - Λ correlations studied via femtoscopy in pp reactions at $\sqrt{s} = 7$ TeV”, *Phys. Rev.* **C99** (2019) 024001, [arXiv:1805.12455](#) [[nucl-ex](#)].
- [34] ALICE Collaboration, S. Acharya et al., “First Observation of an Attractive Interaction between a Proton and a Cascade Baryon”, *Phys. Rev. Lett.* **123** (2019) 112002, [arXiv:1904.12198](#) [[nucl-ex](#)].
- [35] ALICE Collaboration, S. Acharya et al., “Investigation of the p- Σ^0 interaction via femtoscopy in pp collisions”, *Phys. Lett. B* **805** (2020) 135419, [arXiv:1910.14407](#) [[nucl-ex](#)].
- [36] ALICE Collaboration, S. Acharya et al., “Study of the Λ - Λ interaction with femtoscopy correlations in pp and p-Pb collisions at the LHC”, *Phys. Lett. B* **797** (2019) 134822, [arXiv:1905.07209](#) [[nucl-ex](#)].
- [37] ALICE Collaboration, S. Acharya et al., “Unveiling the strong interaction among hadrons at the LHC”, *Nature* **588** no. 7837, (2020) 232–238, [arXiv:2005.11495](#) [[nucl-ex](#)].
- [38] ALICE Collaboration, S. Acharya et al., “Scattering Studies with Low-Energy Kaon-Proton Femtoscopy in Proton-Proton Collisions at the LHC”, *Phys. Rev. Lett.* **124** (2020) 092301.
- [39] ALICE Collaboration, S. Acharya et al., “Constraining the $\bar{K}N$ coupled channel dynamics using femtoscopy correlations at the LHC”, *Eur.Phys.J.C* **83** (5, 2022), [arXiv:2205.15176](#) [[nucl-ex](#)].
- [40] ALICE Collaboration, S. Acharya et al., “Exploring the NA – NE coupled system with high precision correlation techniques at the LHC”, *Phys. Lett. B* **833** (2022) 137272, [arXiv:2104.04427](#) [[nucl-ex](#)].
- [41] ALICE Collaboration, S. Acharya et al., “Investigating the role of strangeness in baryon–antibaryon annihilation at the LHC”, *Phys. Lett. B* **829** (2022) 137060, [arXiv:2105.05190](#) [[nucl-ex](#)].
- [42] ALICE Collaboration, “First measurement of the Λ - Ξ interaction in proton-proton collisions at the LHC”, [arXiv:2204.10258](#) [[nucl-ex](#)].
- [43] ALICE Collaboration, “Future high-energy pp programme with ALICE”.
- [44] ALICE Collaboration, “Letter of intent for ALICE 3: A next-generation heavy-ion experiment at the LHC”, [arXiv:2211.02491](#) [[physics.ins-det](#)].
- [45] M. A. Lisa, S. Pratt, R. Soltz, and U. Wiedemann, “Femtoscopy in relativistic heavy ion collisions”, *Ann. Rev. Nucl. Part. Sci.* **55** (2005) 357–402, [arXiv:nucl-ex/0505014](#).
- [46] J. Haidenbauer, “Coupled-channel effects in hadron-hadron correlation functions”, *Nucl. Phys.* **A981** (2019) 1–16, [arXiv:1808.05049](#) [[hep-ph](#)].
- [47] Y. Kamiya, T. Hyodo, K. Morita, A. Ohnishi, and W. Weise, “ K^-p Correlation Function from High-Energy Nuclear Collisions and Chiral SU(3) Dynamics”, *Phys. Rev. Lett.* **124** no. 13, (2020) 132501, [arXiv:1911.01041](#) [[nucl-th](#)].
- [48] ALICE Collaboration, S. Acharya et al., “Search for a common baryon source in high-multiplicity pp collisions at the LHC”, *Phys. Lett. B* **811** (2020) 135849, [arXiv:2004.08018](#) [[nucl-ex](#)].
- [49] D. Mihaylov and J. González González, “Novel model for particle emission in small collision systems”, *Eur. Phys. J. C* **83** no. 7, (2023) 590, [arXiv:2305.08441](#) [[hep-ph](#)].
- [50] A. Feijoo, D. Gazda, V. Magas, and A. Ramos, “The K^-N Interaction in Higher Partial Waves”, *Symmetry* **13** no. 8, (2021) 1434, [arXiv:2107.10560](#) [[hep-ph](#)].
- [51] A. Ramos, A. Feijoo, and V. K. Magas, “The chiral $S = -1$ meson–baryon interaction with new constraints on the NLO contributions”, *Nucl. Phys. A* **954** (2016) 58–74, [arXiv:1605.03767](#) [[nucl-th](#)].

- [52] L. Fabbietti, V. M. Sarti, and O. V. Doce, “Study of the strong interaction among hadrons with correlations at the LHC”, *Ann. Rev. Nucl. Part. Sci.* **71** (2021) 377–402, [arXiv:2012.09806 \[nucl-ex\]](#).
- [53] ALICE Collaboration, S. Acharya *et al.*, “First study of the two-body scattering involving charm hadrons”, *Phys. Rev. D* **106** no. 5, (2022) 052010, [arXiv:2201.05352 \[nucl-ex\]](#).
- [54] V. Vovchenko, B. Dönigus, and H. Stoecker, “Canonical statistical model analysis of pp, p–Pb, and Pb–Pb collisions at energies available at the CERN Large Hadron Collider”, *Phys. Rev. C* **100** no. 5, (2019) 054906, [arXiv:1906.03145 \[hep-ph\]](#).
- [55] ALICE Collaboration, “Accessing the strong interaction between Λ baryons and charged kaons with the femtoscopy technique at the LHC.” HEPData (collection), 2023. <https://doi.org/10.17182/hepdata.143518>.
- [56] Particle Data Group Collaboration, R. L. Workman *et al.*, “Review of Particle Physics”, *PTEP* **2022** (2022) 083C01.
- [57] J. A. Oller and U. G. Meissner, “Chiral dynamics in the presence of bound states: Kaon nucleon interactions revisited”, *Phys. Lett. B* **500** (2001) 263–272, [arXiv:hep-ph/0011146](#).
- [58] B. Borasoy, R. Nissler, and W. Weise, “Chiral dynamics of kaon-nucleon interactions, revisited”, *Eur. Phys. J. A* **25** (2005) 79–96, [arXiv:hep-ph/0505239](#).
- [59] Z.-H. Guo and J. A. Oller, “Meson-baryon reactions with strangeness -1 within a chiral framework”, *Phys. Rev. C* **87** no. 3, (2013) 035202, [arXiv:1210.3485 \[hep-ph\]](#).
- [60] A. Feijoo, V. Magas, and A. Ramos, “ $S=-1$ meson-baryon interaction and the role of isospin filtering processes”, *Phys. Rev. C* **99** no. 3, (2019) 035211, [arXiv:1810.07600 \[hep-ph\]](#).
- [61] W. H. Press, S. A. Teukolsky, W. T. Vetterling, and B. P. Flannery, *Numerical Recipes in C*. Cambridge University Press, Cambridge, USA, second ed., 1992.
- [62] B. Efron and R. Tibshirani, “An introduction to the bootstrap”, *Statist. Sci.* **57** no. 1, (1986) 54–75.
- [63] M. Albaladejo, D. Jido, J. Nieves, and E. Oset, “ $D_{s0}^*(2317)$ and DK scattering in B decays from BaBar and LHCb data”, *Eur. Phys. J. C* **76** no. 6, (2016) 300, [arXiv:1604.01193 \[hep-ph\]](#).
- [64] E. Braaten and H. W. Hammer, “Universality in few-body systems with large scattering length”, *Phys. Rept.* **428** (2006) 259–390, [arXiv:cond-mat/0410417](#).
- [65] P. Naidon and S. Endo, “Efimov Physics: a review”, *Rept. Prog. Phys.* **80** no. 5, (2017) 056001, [arXiv:1610.09805 \[quant-ph\]](#).
- [66] T. Hyodo, “Structure of Near-Threshold s-Wave Resonances”, *Phys. Rev. Lett.* **111** (2013) 132002, [arXiv:1305.1999 \[hep-ph\]](#).
- [67] F. Giacosa, A. Okopińska, and V. Shastry, “A simple alternative to the relativistic Breit–Wigner distribution”, *Eur. Phys. J. A* **57** no. 12, (2021) 336, [arXiv:2106.03749 \[hep-ph\]](#).